Depression of Nonlinearity in Decaying Isotropic MHD Turbulence

S. Servidio,[1] W. H. Matthaeus,[1] and P. Dmitruk[1,2]

[1]*Bartol Research Institute and Department of Physics and Astronomy, University of Delaware, Newark, Deleware 19716, USA*
[2]*Departmento de Física, Facultad de Ciencias Exactas y Naturales, Universidad de Buenos Aires, Ciudad Universitaria, 1428, Buenos Aires, Argentina*

(Received 9 October 2007; published 7 March 2008)

Spectral method simulations show that undriven magnetohydrodynamic turbulence spontaneously generates coherent spatial correlations of several types, associated with local Beltrami fields, directional alignment of velocity and magnetic fields, and antialignment of magnetic and fluid acceleration components. These correlations suppress nonlinearity to levels lower than what is obtained from Gaussian fields, and occur in spatial patches. We suggest that this rapid relaxation leads to non-Gaussian statistics and spatial intermittency.

DOI: 10.1103/PhysRevLett.100.095005 PACS numbers: 52.30.Cv, 52.35.Bj, 52.35.Ra, 96.50.Tf

Two central features of magnetohydrodynamic (MHD) turbulence are generally studied independently: the production of intermittency and the appearance of distinctive states associated with turbulent relaxation. It is, for example, well known that the random phase approximation fails as a turbulence description in that it cannot produce non-Gaussian statistics, such as high kurtosis of vorticity and current, multifractal scaling of moments, and other signatures of intermittency [1]. On the other hand, MHD relaxation theory has led to notable successes associated with Taylor relaxation, selective decay, global dynamic alignment, and helical dynamo action [2–5]. Relaxation is most often viewed as a long-time consequence of multiple global ideal conservation principles, or global maximization of entropy. In a few cases [6,7], relaxation has been shown to act locally and rapidly, with clear consequence for the statistics of the turbulence. Here, we further explore several rapid relaxation processes which are necessarily local and that occur rapidly and simultaneously. These lead to force free magnetic fields, directionally aligned velocity and magnetic fields, anticorrelation between advection and Lorentz forces and between magnetic acceleration components. The net effect in all cases is a reduction of the strength of nonlinearity to levels substantially below that associated with uncorrelated Gaussian primitive fields.

Previous studies of incompressible hydrodynamic (NS) turbulence demonstrate that nonlinear evolution leads to aligned velocity ($\boldsymbol{v}$) and vorticity ($\boldsymbol{\omega}$) fields in regions of low dissipation [6–8]. Subsequent study [6] revealed that this alignment is associated with systematic depression of the strength of nonlinear couplings relative to values obtained with a Gaussian-distributed velocity field having the same velocity spectrum. Therefore, arguably the localization of kinetic helicity due to this ''beltramization'' [6,7,9] is related to coherent structure formation and to small-scale intermittency [10].

Study of the analogous effects in MHD involves both velocity $\boldsymbol{v}$ and magnetic $\boldsymbol{b}$ fields and therefore additional possibilities for correlation and suppression of nonlinearity. In 3D MHD, the Beltrami property of both $\boldsymbol{v}$ and $\boldsymbol{b}$ can be obtained by variational principles that were previously applied to long-time (many turnover times) global relaxation processes [5]. Minimum energy states [4], for 3D spatially periodic MHD, are determined from the variational problem

$$\delta \int [(|\boldsymbol{v}|^2 + |\boldsymbol{b}|^2) - 2\alpha \boldsymbol{v}\cdot\boldsymbol{b} - \phi \boldsymbol{a}\cdot\boldsymbol{b}] d^3x = 0 \qquad (1)$$

where α and ϕ are Lagrange multipliers (for the simplest case taken as constants), $\boldsymbol{a}$ the potential vector, and $\boldsymbol{b} = \boldsymbol{\nabla}\times\boldsymbol{a}$. This equation minimizes incompressible energy $E = \langle|\mathbf{v}|^2 + |\mathbf{b}|^2\rangle/2$ while holding constant the magnetic helicity $H_m = \langle \boldsymbol{a}\cdot\boldsymbol{b}\rangle$ and cross helicity $H_c = \langle \boldsymbol{v}\cdot\boldsymbol{b}\rangle$. Here, $\langle\ldots\rangle$ denotes a spatial average. The kinetic helicity $H_v = \langle \boldsymbol{v}\cdot\boldsymbol{\omega}\rangle$ is not conserved in ideal MHD and is therefore not constrained. The Euler-Lagrange equations imply in the relaxed state that

$$\boldsymbol{v} = \alpha\boldsymbol{b} = \frac{\alpha(1-\alpha^2)}{\phi}\boldsymbol{j} = \frac{1-\alpha^2}{\phi}\boldsymbol{\omega}. \qquad (2)$$

A special case is the well-known and entirely magnetic Taylor relaxed state [2], which is ''force free'' in that $\boldsymbol{v} = 0$ and the electric current density $\boldsymbol{j} = \nabla\times\boldsymbol{b}$ is parallel to $\boldsymbol{b}$. When cross helicity is nonzero, Eq. (2) implies that $\boldsymbol{v} \neq 0$, and an Alfvénic solution is described. In this case, the resulting field need not be force free. Globally aligned and equipartitioned *Alfvénic states* are sometimes approximately realized in the solar wind plasma [11].

Why should such states emerge? From the perspective of turbulence theory, Taylor states and their generalizations emerge dynamically as a consequence of relaxation process known as selective decay [5] and dynamic alignment [12]. In this view, constrained energy minimization provide a means, based on the budgets of conserved quadratic ideal invariants, to characterize dynamical evolution toward predictable long-time states [4]. For homogeneous MHD,

turbulence simulations show that a balance is achieved between these two relaxation processes. The result is that the magnetofluid evolves toward long wavelength states dominated by magnetic (possibly helical) excitations in which $\mathbf{v}$ and $\mathbf{b}$ are also highly correlated [4,5]. Typically, global relaxation requires many nonlinear eddy turnover times. Steady, driven MHD also shows alignment at small scales [13].

There has been, prior to this time, little suggestion of the relevance of the above global relaxation picture to turbulence evolution at shorter time scales. Recently, however, it has been shown that local directional alignment of velocity and magnetic fluctuations occurs rapidly in MHD for a variety of parameters in direct numerical simulations and is also seen in solar wind data [14]. Here, we look for rapid relaxation associated with correlations and directional near-alignments of several types. All of these are found to occur in less than one turnover time. These processes suppress nonlinear MHD couplings and need not be associated with global alignment, but rather occur independently, rapidly, and in spatial patches.

We study numerical solutions of the equations of MHD in dimensionless variables

$$\begin{aligned}\frac{\partial \boldsymbol{v}}{\partial t} &= \boldsymbol{v}\times\boldsymbol{\omega} + \boldsymbol{j}\times\boldsymbol{b} - \boldsymbol{\nabla}P^* + R_\nu^{-1}\boldsymbol{\nabla}^2\boldsymbol{v}\\ \frac{\partial \boldsymbol{b}}{\partial t} &= (\boldsymbol{b}\cdot\boldsymbol{\nabla})\boldsymbol{v} - (\boldsymbol{v}\cdot\boldsymbol{\nabla})\boldsymbol{b} + R_\mu^{-1}\boldsymbol{\nabla}^2\boldsymbol{b},\end{aligned} \tag{3}$$

where $\boldsymbol{\nabla}\cdot\boldsymbol{b} = 0$, and R_ν and R_μ are kinetic and magnetic Reynolds numbers. The kinetic pressure $P^* = p + (v^2/2)$ maintains the incompressibility constraint $\nabla\cdot\boldsymbol{v} = 0$. We employ direct undriven Fourier pseudospectral [15] simulations of Eqs. (3) using triply periodic boundary conditions (side $2\pi L$), 128^3 resolution, and $R_\nu = R_\mu = 400$. The scheme ensures ideal continuous time conservation of E, H_m, and H_c. The initial fluctuation amplitudes for $\boldsymbol{v}$ and $\boldsymbol{b}$ have equal mean square values normalized to 1, are nonzero in the wave number shell $1 \le kL \le 4$, and have random phases. The initial H_c, H_v, and H_m are small. Results with nonzero helicities will be presented at a later time.

Our approach parallels studies [6] of suppression of nonlinearity in NS turbulence. We compute the distributions (PDFs) of the angle

$$\cos\theta = \frac{\mathbf{f}\cdot\mathbf{g}}{|\mathbf{f}||\mathbf{g}|} \tag{4}$$

where $\{\mathbf{f},\mathbf{g}\}$ represents one of $\{\boldsymbol{v},\boldsymbol{b}\}$, $\{\boldsymbol{v},\boldsymbol{\omega}\}$, $\{\boldsymbol{j},\boldsymbol{b}\}$, and $\{\boldsymbol{j},\boldsymbol{\omega}\}$. In Fig. 1, these four PDFs are shown. The initial Gaussian distribution with null (net) helicities corresponds to imposing a flat initial distribution of Eq. (4). Quickly, as the nonlinearity develops, strong alignments appear. These aligned (antialigned) fields correspond to a beltramization of the magnetofluid, similar to the NS case. Even though global helicities remain small, the magnetofluid locally self-organizes into patches (not shown here) which contain several types of correlations.

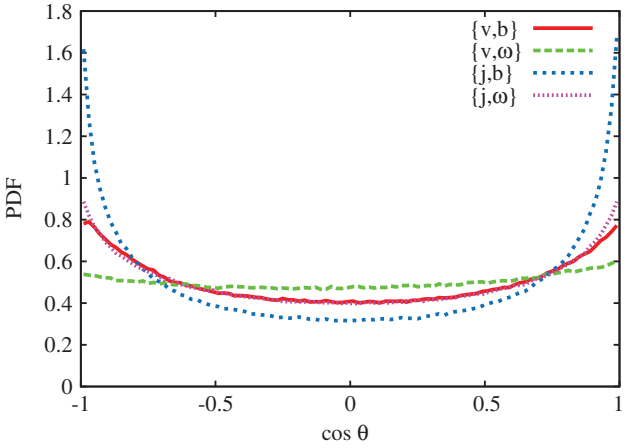

FIG. 1 (color). PDF of Eq. (4) for the sets of fields: $\{\boldsymbol{v},\boldsymbol{b}\}$ (red), $\{\boldsymbol{v},\boldsymbol{\omega}\}$ (green), $\{\boldsymbol{j},\boldsymbol{b}\}$ (blue), $\{\boldsymbol{j},\boldsymbol{\omega}\}$ (pink). The PDFs are evaluated at $t = 2.0\tau_A$ (Alfvèn time τ_A).

The level of alignment can be explored by computing the following quantities [6]:

$$C_{\mathbf{f},\mathbf{g}} = \frac{\langle|\mathbf{f}\times\mathbf{g}|^2\rangle}{\langle|\mathbf{f}|^2\rangle\langle|\mathbf{g}|^2\rangle}; \qquad D_{\mathbf{f},\mathbf{g}} = \frac{\langle|\mathbf{f}\cdot\mathbf{g}|^2\rangle}{\langle|\mathbf{f}|^2\rangle\langle|\mathbf{g}|^2\rangle}. \tag{5}$$

By randomizing the fields $\mathbf{f}$ and $\mathbf{g}$ with Gaussian distributions while retaining the same (average) spectrum, we arrive at the corresponding "Gaussianized" fields $\mathbf{f}^G$ and $\mathbf{g}^G$. Then we can compute $D'_{\mathbf{f},\mathbf{g}} = D_{\mathbf{f},\mathbf{g}}/D_{\mathbf{f}^G,\mathbf{g}^G}$ which is a measure of the degree of alignment with respect to the phase-randomized reference field. Analogously, we compute $C'_{\mathbf{f},\mathbf{g}} = C_{\mathbf{f},\mathbf{g}}/C_{\mathbf{f}^G,\mathbf{g}^G}$. The time behavior of C' and D' for several field couples is shown in Fig. 2. The level of alignment is different for each set of fields: It is stronger for $\{\boldsymbol{j},\boldsymbol{b}\}$ and for $\{\boldsymbol{v},\boldsymbol{b}\}$ compared to $\{\boldsymbol{v},\boldsymbol{\omega}\}$. The stronger

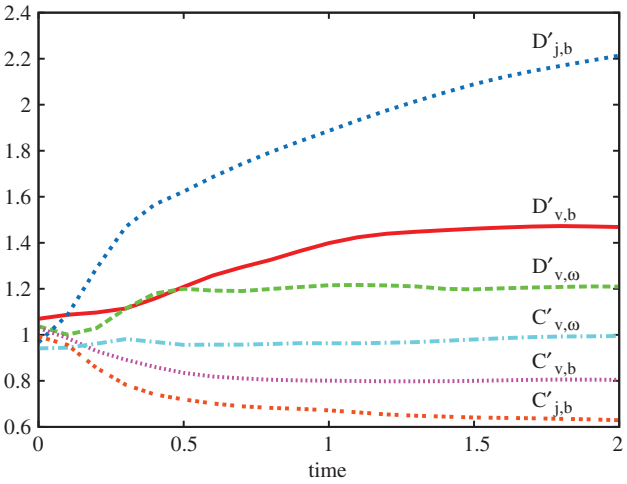

FIG. 2 (color). Time history of the ratio of the alignment measures to their Gaussian values, $D'_{\mathbf{f},\mathbf{g}} = D_{\mathbf{f},\mathbf{g}}/D_{\mathbf{f}^G,\mathbf{g}^G}$ and $C'_{\mathbf{f},\mathbf{g}} = C_{\mathbf{f},\mathbf{g}}/C_{\mathbf{f}^G,\mathbf{g}^G}$ (see text) for $\{\mathbf{f},\mathbf{g}\} = \{\boldsymbol{v},\boldsymbol{b}\}$, $\{\boldsymbol{v},\boldsymbol{\omega}\}$, $\{\boldsymbol{j},\boldsymbol{b}\}$.

correlations are those related to quantities (H_m and H_c) that are conserved by nonlinear activity apart from transport across internal boundaries.

Increased probability of occurrence of Beltrami correlations ($\cos\theta = \pm 1$) appears to be associated with rapid adjustments of the turbulence that occur as a response to nonlinear forces, leading to regions in which the nonlinear term has become suppressed and the energy cascade has become inhibited [8]. Alignment is not destroyed in these regions in part because of the conservation of H_m and H_c. On the other hand, for MHD, H_v is not conserved, and consequently the level of alignment of $\{\boldsymbol{v}, \boldsymbol{\omega}\}$, in contrast with the NS case, is small, while alignments of $\{\boldsymbol{j}, \boldsymbol{b}\}$ and of $\{\boldsymbol{v}, \boldsymbol{b}\}$ (and indirectly $\{\boldsymbol{j}, \boldsymbol{\omega}\}$) are maintained at larger levels.

We also look at balance between advection $\boldsymbol{F}_A = (\boldsymbol{v} \times \boldsymbol{\omega})^*$ and Lorentz $\boldsymbol{F}_L = (\boldsymbol{j} \times \boldsymbol{b})^*$ forces. (The asterisks $*$ denote the solenoidal part, obtained by k-space projection. This eliminates forces that are cancelled by the pressure term.) A similar analysis is performed for the magnetic accelerations $\boldsymbol{F}_{b1} = [(\boldsymbol{b} \cdot \boldsymbol{\nabla})\boldsymbol{v}]$ and $\boldsymbol{F}_{b2} = [(\boldsymbol{v} \cdot \boldsymbol{\nabla})\boldsymbol{b}]$. Several variations of this analysis, not shown, provide similar results. The hypothesis outlined above, that rapid adjustments reduce accelerations, can be further explored with regard to these terms. Figure 3 shows that these contributions to the momentum and magnetic accelerations become strongly antialigned. This phenomenon, that we named *secondary alignment*, is manifest in strongly skewed PDFs of $\boldsymbol{F}_A \cdot \boldsymbol{F}_L$ and $\boldsymbol{F}_{b1} \cdot \boldsymbol{F}_{b2}$. This is another signature of the cancellation of accelerations, or suppression of nonlinearity, following Kraichnan's terminology. Indeed, from Eqs. (3), the production of local Beltrami flows, along with the emergent anticorrelation of acceleration components, causes a reduction of (generalized) acceleration, as we now show.

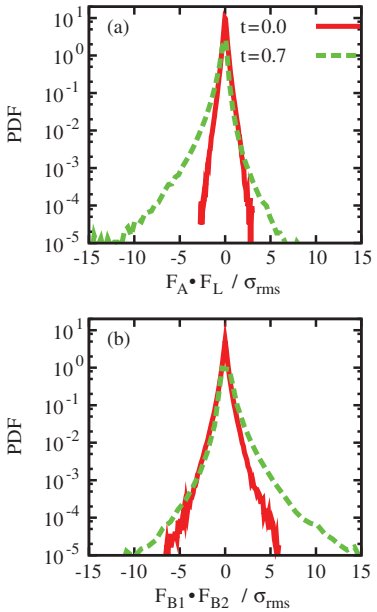

FIG. 3 (color). PDFs normalized to the rms value for: (a) "$\boldsymbol{F}_A \cdot \boldsymbol{F}_L$," (b) "$\boldsymbol{F}_{b1} \cdot \boldsymbol{F}_{b2}$," at $t = 0$ (red) and $t = 0.7\tau_A$ (green).

To quantify suppression of nonlinearity in the momentum and the magnetic induction equations, we introduce

$$Q = \frac{\sqrt{\langle |\mathbf{F}_A + \mathbf{F}_L|^2 \rangle}}{\sqrt{\langle |\mathbf{F}_A|^2 \rangle} + \sqrt{\langle |\mathbf{F}_L|^2 \rangle}}; \qquad M = \frac{\sqrt{\langle |[\mathbf{F}_{b1} - \mathbf{F}_{b2}|^2 \rangle}}{\sqrt{\langle |\mathbf{F}_{b1}|^2 \rangle} + \sqrt{\langle |\mathbf{F}_{b2}|^2 \rangle}}, \tag{6}$$

where we use simple geometric considerations to define these diagnostics: $|Q| \leq 1$ and $|M| \leq 1$ by a triangle inequality. We computed the ratios $Q' = Q/Q_G$ and $M' = M/M_G$ in analogy to the discussion following Eq. (5). Q_G and M_G are computed from Eq. (6) using the corresponding Gaussianized fields. We do not include viscous or resistive dissipation in the above diagnostics as these can modify wave number spectra, but cannot introduce phase correlations of the type responsible for the observed alignments. As reported in Fig. 4(a), the strength of momentum and magnetic nonlinearities are reduced to $\sim$86% and $\sim$92%, respectively, of their Gaussianized values. In both cases, the ratio decreases and reaches a minimum after $\simeq 0.7\tau_A$. An analogous minimum (peak) is observed in the antialignment of $\{\boldsymbol{F}_A, \boldsymbol{F}_L\}$ and $\{\boldsymbol{F}_{b1}, \boldsymbol{F}_{b2}\}$. In Fig. 4(b), the skewness as a function of time, for PDFs of Fig. 3, is reported. The skewness is maximum simultaneously with the level of the depression, and there is a suggestion of a major contribution to the suppression from the secondary alignment.

In order to show the direct relation between this suppression of nonlinearity and intermittency, we computed time histories of the kurtosis of the electric current density (K_j) and the vorticity (K_ω). In Fig. 4(c), the values of K_j and K_ω, evaluated for the x component, are shown. Because of the isotropy of the system, all components have the same behavior. This quantity is an elementary measure of the degree of the intermittency of the system. The skewness and the mean accelerations have peaks at

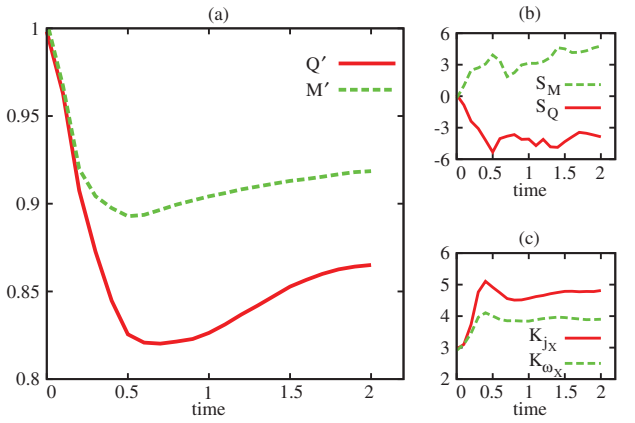

FIG. 4 (color). (a) $Q' = Q/Q_G$ (red) and $M' = M/M_G$ (green). (b) Skewness of PDF of $\boldsymbol{F}_A \cdot \boldsymbol{F}_L$ (red) and $\boldsymbol{F}_{b1} \cdot \boldsymbol{F}_{b2}$ (green). (c) Kurtosis for x component of current (red), vorticity (green).

more or less the same time, suggesting that the degree of beltramization is strongly related to the appearance of intermittent structures. The interpretation is that the emergence of alignment, the Beltrami property and cancellation leads rapidly to local regions in which the nonlinearity is weak, thus concentrating nonlinear stresses near boundaries of these regions. The release of these stresses near the patch boundaries is associated with generation of small-scale gradients, e.g., current or vortex sheets, which more or less define these sharp boundaries, providing signatures of intermittency. Thus, rapid relaxation leads to suppression of nonlinearity and also to the generation of intermittency.

We conclude that the nonlinear dynamics of decaying, isotropic, 3D incompressible MHD leads spontaneously to a complex picture where several kind of alignments appear. MHD turbulence produces a hierarchy of several rapid, local relaxation processes, favoring states having strong alignments or antialignments between $\{\boldsymbol{v}, \boldsymbol{b}\}$ (Alfvénic states), $\{\boldsymbol{j}, \boldsymbol{b}\}$ (force free), $\{\boldsymbol{j}, \boldsymbol{\omega}\}$ and more weakly $\{\boldsymbol{v}, \boldsymbol{\omega}\}$. This process is not related directly to long terms relaxation processes, since, even if the global alignment is null ($H_c = H_v = H_m \simeq 0$), the distribution of the cosine of the angle between these quantities becomes rapidly peaked near ± 1. Moreover, we found an additional local relaxation that also reduces the strength of nonlinearity—that is, a high level of cancellation between fluid accelerations produced by mechanical and magnetic stresses, and between magnetic accelerations produced by advection and field line stretching. Clearly, the multiplicity of nonlinear terms in MHD tends to a self-organization in such a way that the total forces are strongly damped and, consequently, the amplitude of accelerations reduces drastically. The level of depression is different for Q and M. This phenomenon may be related to the tendency of MHD to produce a high level of magnetic energy relative to kinetic energy [4]. In our simulation, the Alfvènic ratio E_v/E_b reduced from one (at $t = 0$) to $\simeq 0.65$ (at $t = 2\tau_A$).

The production of these spatial patches of correlations and anticorrelations requires that the statistical distribution of velocity and magnetic field become non-Gaussian, in particular, because each type of relaxation requires that at least the fourth order correlations become non-Gaussian. Our conclusion is that this multifaceted rapid relaxation is intimately related to the formation of spatial intermittent structures. A simple real space picture emerges: when patches of suppression of nonlinearity are formed, the fourth order statistics become non-Gaussian, as the gradients become concentrated along boundaries of the patches. For example, two regions can become approximately force free, but the boundary between them will not be force free [16]. Localized nonlinear couplings can further enhance gradients in these boundary regions. Magnetic reconnection is one example of the type activity that can occur at these boundaries. We therefore suggest that the key to understanding intermittency statistics in MHD may be to further understand how rapid suppression of nonlinearity occurs. For example, it may be possible to represent such patchy relaxation by revisiting solutions to Eq. (1) with space-dependent Lagrange multipliers.

Further numerical and analytical work is required to understand the level of suppression of nonlinearity, and how this might vary with turbulence parameters, for example, with the Alfvèn ratio, the Reynolds numbers, and the presence of forcing. We also suspect that arguments might be developed, perhaps based on a local entropic principle, in which relaxation along the lines of Eq. (1) emerges locally. Recognition of these rapid forms of local MHD relaxation will likely lead to further insights into the dynamical evolution of MHD turbulence, as well as the nature of intermittency in the evolution of strongly dynamical fluid plasmas in space and astrophysics.

We thank P. Mininni and A. Pouquet for useful discussions. This research is supported in part by NSF Grant No. ATM0539995 and NASA under No. NNG05GG83G, subcontract No. LANL-11748-001-05, and the Heliophysics Theory Program. P. D. is a member of Carrera Investigador Cientifico of CONICET.

[1] U. Frisch, *Turbulence: The Legacy of A.N. Kolmogorov* (Cambridge U. Press, Cambridge, England, 1995).
[2] J. B. Taylor, Phys. Rev. Lett. **33**, 1139 (1974).
[3] P. D. Mininni, D. O. Gómez, and S. M. Mahajan, Astrophys. J. **567**, L81 (2002).
[4] T. Stribling and W. H. Matthaeus, Phys. Fluids B **3**, 1848 (1991); S. Ohsaki and Z. Yoshida, Phys. Plasmas **12**, 064505 (2005); A. C. Ting, D. Montgomery, and W. H. Matthaeus, Phys. Fluids **29**, 3261 (1986).
[5] D. Montgomery, L. Turner, and G. Vahala, Phys. Fluids **21**, 757 (1978); W. H. Matthaeus and D. Montgomery, Ann. N.Y. Acad. Sci. **357**, 203 (1980); P. D. Mininni, D. Montgomery, and A. Pouquet, Phys. Fluids **17**, 035112 (2005).
[6] R. H. Kraichnan and R. Panda, Phys. Fluids **31**, 2395 (1988).
[7] R. B. Pelz, V. Yakhot, S. A. Orszag, L. Shtilman, and E. Levich, Phys. Rev. Lett. **54**, 2505 (1985).
[8] R. M. Kerr, Phys. Rev. Lett. **59**, 783 (1987).
[9] Wm. T. Ashurst, A. R. Kerstein, R. M. Kerr, and C. H. Gibson, Phys. Fluids **30**, 2343 (1987).
[10] H. K. Moffat, *Turbulence and Chaotic Phenomena in Fluids* (North-Holland, Amsterdam, 1984).
[11] J. W. Belcher and L. Davis, Jr., J. Geophys. Res. **76**, 3534 (1971).
[12] M. Dobrowolny, A. Mangeney, and P. Veltri, Phys. Rev. Lett. **45**, 144 (1980).
[13] J. Mason *et al.*, Phys. Rev. Lett. **97**, 255002 (2006); S. Boldyrev, Phys. Rev. Lett. **96**, 115002 (2006).
[14] W. H. Matthaeus, A. Pouquet, P. D. Mininni, P. Dmitruk, and B. Breech, Phys. Rev. Lett. (to be published).
[15] S. Ghosh, M. Hossain, and W. H. Matthaeus, Comput. Phys. Commun. **74**, 18 (1993).
[16] M. R. Brown, J. Plasma Phys. **57**, 203 (1997).